

APPLICATION OF PERCOLATION THEORY AND FRACTAL GEOMETRY TO TABLET COMPACTION

H. Leuenberger, R. Leu and J.D. Bonny
School of Pharmacy, University of Basle,
Totengaesslein 3, CH-4051 Basle, Switzerland

SUMMARY

Percolation theory¹ and fractal geometry² represent novel powerful concepts which cover a wide range of applications in pharmaceutical technology³. Both concepts provide new insights into the physics of tablet compaction and the properties of compacts⁴⁻¹¹. The paper reviews and summarizes the most recent findings in the application of percolation theory and fractal geometry to tablet compaction which include four sections i.e. 1) short introduction to percolation theory and fractal geometry, 2) the formation of a tablet^{4,7,10}, 3) tablet properties such as deformation hardness, tensile strength¹⁰ and 4) drug dissolution from a matrix type controlled release system^{3,9,11}.

SHORT INTRODUCTION TO PERCOLATION THEORY AND FRACTAL GEOMETRY

Percolation Theory

Different types of percolation can be distinguished: random-site, random-bond, random-site-bond, correlate chain, etc. Generally, percolation theory deals with the number and properties of clusters¹. A percolation system is considered to consist of sites in an infinitely large real or virtual lattice. Applying the principles of random-site percolation to a particulate system, a cluster may be considered as a single particle or a group of similar particles which occupy bordering sites in the particulate system. In the case of bond percolation, a group of particles is considered to belong to the same cluster only when bonds are formed between neighboring particles (see figs. 1a and 1b).

In random-bond percolation, the bond probability and bond strength between different components can play an important role. The bond probability p can assume values between 0 and 1. When $p = 1$, all possible bonds are formed and the tablet strength is at its maximum, i.e. a tablet should show maximal strength at zero porosity when all bonds are formed. In order to form a

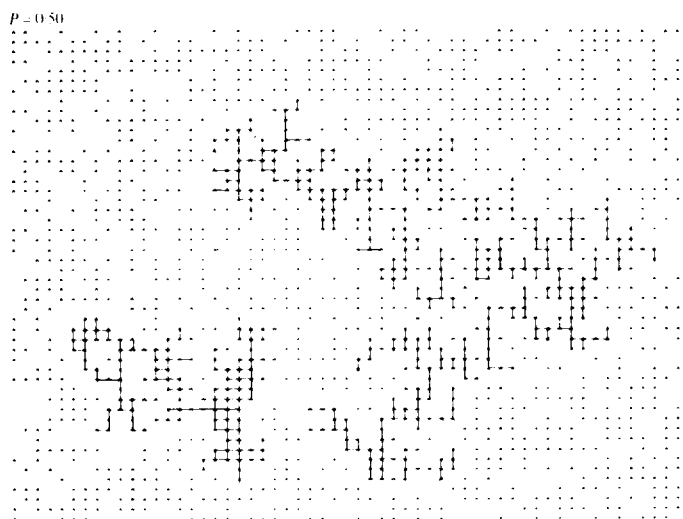


FIGURE 1a

Example for percolation on a 60 x 60 square lattice for $p = 0,50^1$. Occupied sites are shown as "*", empty sites are ignored. Two clusters are marked by bonds.

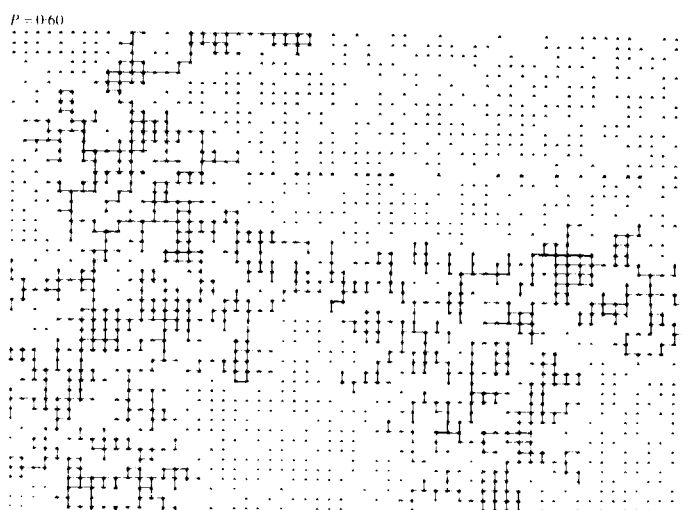


FIGURE 1b

Example for percolation on a 60 x 60 square lattice for $p = 0,60^1$. The "infinite cluster" is marked by bonds.

stable compact it is necessary that the bonds percolate to form an "infinite" cluster within the ensemble of powder particles filled in a die and put under compressional stress.

Site percolation is an important model of a binary mixture consisting of two different materials. In the three-dimensional case, two percolation thresholds, p_c , can be defined: a lower threshold, p_{c1} , where one of the components just begins to percolate, and a second upper percolation threshold, p_{c2} , where the other component ceases to have an infinite cluster. Between the two thresholds the two components form two interpenetrating percolating networks. Below the lower respectively above the upper percolation threshold, the clusters of the corresponding components are finite and isolated. Thus, in site percolation of a binary powder mixture, p_c corresponds to a critical concentration ratio of the two components. From emulsion systems these concentrations are well known where oil-in-water or water-in-oil emulsions can be prepared exclusively.

Table 1 shows critical volume-to-volume ratios for well-defined geometrical packing of monosized spherical particles. The critical volume-to-volume ratios depend on the type of percolation and the type of lattice. In the case of real powder systems the geometrical packing

TABLE 1

Selected Percolation Thresholds for Three-Dimensional Lattices¹

| Lattice type | Site | Bond |
|---------------------|-------|-------|
| Diamond | 0.428 | 0.388 |
| Simple cubic | 0.312 | 0.249 |
| Body-centered cubic | 0.245 | 0.179 |
| Face-centered cubic | 0.198 | 0.119 |

is a function of the particle size, the particle size distribution and the shape of the particles.

As different types of packing of monosized spherical particles show different porosities, a powder system which has the porosity ϵ can be represented in an idealized manner as an ensemble of monosized spheres having the hypothetical mean diameter x and a mean coordination number k corresponding to hypothetical (idealized) geometrical packing. Table 2 shows the coordination number of isometric spherical particles of different packing structures.

Using the simplified model of powder systems mentioned, the following equation was developed¹²:

$$k = \pi/\epsilon \quad (1)$$

for porosities in the range

$$0.25 < \epsilon < 0.5$$

TABLE 2

Coordination Numbers of Isometric Spherical Particles
for Different Packing Structures

| Lattice type | Coordination number | Porosity |
|---------------------|---------------------|----------|
| Diamond | 4 | 0.66 |
| Simple cubic | 6 | 0.48 |
| Body-centered cubic | 8 | 0.32 |
| Face-centered cubic | 12 | 0.26 |

This equation is a rough estimate and does not hold for compacts, where ϵ usually is less than 0.25.

At a percolation threshold some property of a system may change abruptly or may suddenly become evident. Such an effect starts to occur close to p_c and is usually called a critical phenomenon. As an example, the electrical conductivity of a tablet consisting of copper powder mixed with Al_2O_3 powder may be cited. The tablet conducts electricity only if the copper particles form an "infinite" cluster within the tablet, spanning the tablet in all three dimensions.

In case of a pharmaceutical tablet consisting of an active drug substance and excipients the principle of function is not the electric conductivity and the tablet usually does not consist of a binary powder system compressed. However, often also in case of a complex tablet composition the system can be reduced to

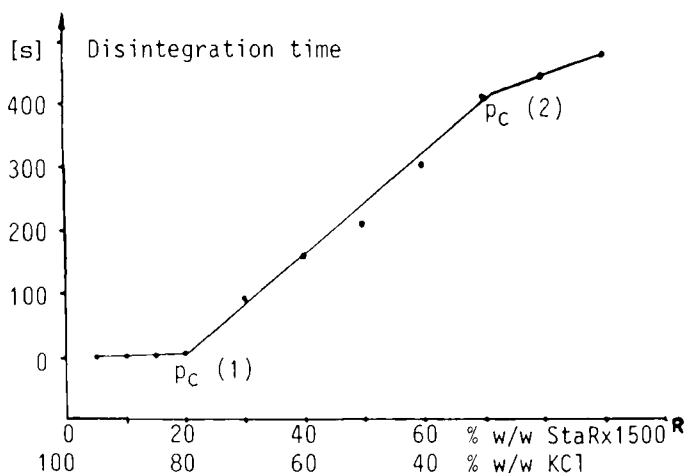


FIGURE 2

Percolation thresholds for the compacted binary mixture KCl-StaRX 1'500^R; Tablet property: disintegration time.

a type of binary powder system dividing the drug and excipients etc. involved in two classes of function, e.g. material which is swelling or is easily dissolved in water. Thus in case of a mixture KCl-StaRX 1500^R cornstarch the two percolation thresholds expected are well recognised as a function of the disintegration time of the tablet (see fig. 2).

Fractal Geometry

Fractal geometry is related to the principle of self-similarity, i.e. the geometrical shape is kept identical independent of the scale, magnification or power of resolution². In practice the range of self-

similarity may however sometimes be limited to only a few orders of magnitude. A typical case of fractal geometry is the so called Coastline of Britain Problem²: the length of the coastline is continuously increasing with increasing power of resolution, i.e. with a smaller yardstick to measure the length. Thus a log-log plot of the length of the coastline as a function of the length of the yardstick to perform a polygon approximation yields a straight line with the slope $(1-D_f)$ with D_f equal to the fractal dimension. Coastlines with perfect self-similarity can be also constructed mathematically (see fig. 3). The fractal dimension of a coastline is thus in between the Euclidean dimension 1 for a straight line and 2 for a surface. It is also fruitful to imagine a fractal surface dimension D_s describing the roughness of a surface. Such a description again includes the prerequisite of a self-similar shape independent of the scale. In this respect the introduction of a surface fractal is very advantageous in powder technology: the result of a measurement of the specific surfaces of a powder is - as it is well known - dependent on the power of resolution of the apparatus (e.g. Blaine, mercury intrusion porosimetry, nitrogen gas adsorption BET-method etc.). Thus the result of a measurement with a chosen method is not able to describe adequately the

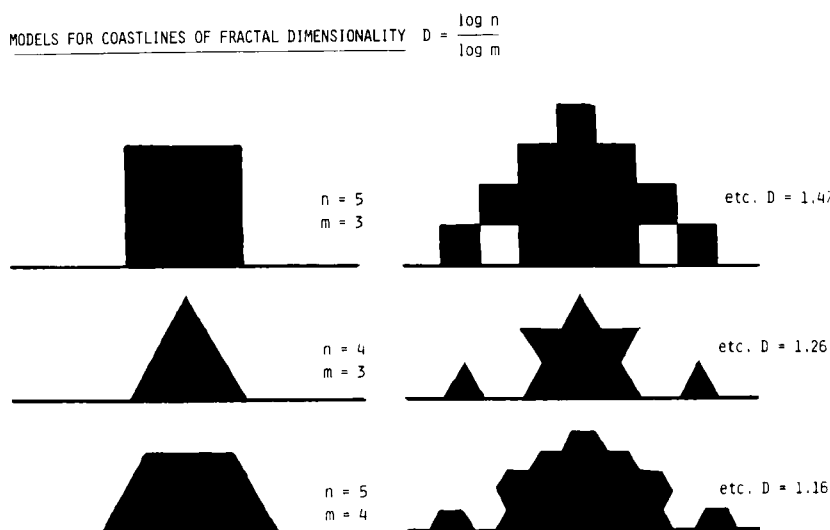


FIGURE 3

Different self-similar structures as coastline models, m = theoretical number of equal parts of the unit length projected on a straight line, n = theoretical number of equal parts of unit length describing the coastline structure.

roughness of the surface. However, if this roughness shows at least within a certain range an approximative self-similarity it is possible to describe the surface by indicating a value for the specific surface and a value for the surface fractal D_s . Consequently, it is possible to know the specific surface data for different powers of resolution applying a log-log plot of the specific surface as a function of the yardstick length, describing the power of resolution, where the slope of the resulting straight line is equal to $2 - D_s$. As the slope is negative, i.e. a surface is higher for

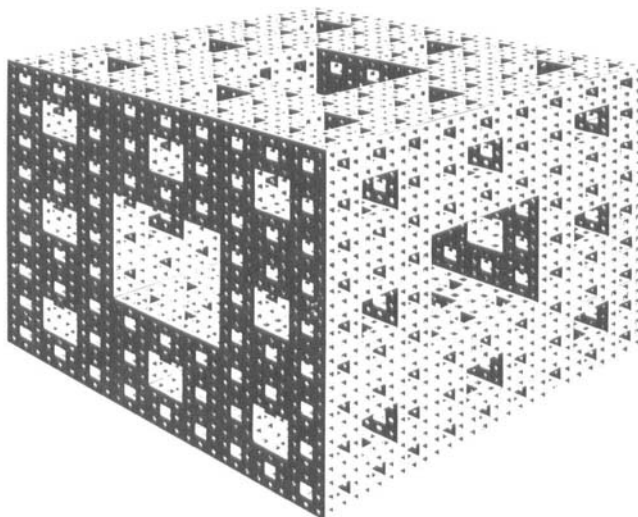


FIGURE 4

Menger sponge with fractal dimension of 2,73 (idealized three-dimensional network of a pore system).

a smaller yardstick length, the value for D_s is between 2 and 3. In case of porous material it is also possible to define a volume fractal. This concept is based on the fact that as a function of the power of resolution to detect a pore volume or pore size the void volume is increased. It is evident that in a practical case the porosity of a material attains a limiting value, i.e. the self-similarity principle is only valid within a limited range. Based on a mathematical self-similar model of pores, i.e. a Menger sponge (see fig. 4) the relationship between the accessible void space (sum of pore volumes) and the power of resolution of the pore

size was established⁹. For this purpose the mercury intrusion porosimetry is the method of choice as the pore volume, i.e. the void space of a tablet is filled with mercury as a function of the mercury intrusion pressure, which is related to the accessible pore size. It is, however, necessary to keep in mind that as a consequence of percolation theory not all of the pores are accessible in the same way and some of them are not accessible at all, i.e. there may be closed pores present and pores of increased size may be hidden behind pores of smaller size, a fact that is responsible for the hysteresis loop between filling-up and draining-off the mercury from the void space within the tablet. These reservations have to be taken into account when the volume fractal dimension of D_v of a porous network is determined.

In case of a porous network the solid fraction, i.e. relative density $\rho_r = 1 - \epsilon$ of the tablet, determined according to the pore volume fraction ϵ (d) filled-up by mercury as function of the pore diameter d is related to the volume fractal D_v as follows

$$\log \rho_r = (3 - D_v) \log d + c \quad (2)$$

with $c = \text{constant}$.

It is a unique property of the Menger sponge that its surface and volume fractal D_s and D_v are identical and equal to $2.727 = \log 20 / \log 3$.

On the other hand, in case of an agglomerate or aggregate of the size L consisting of identical primary particles of diameter δ the following relationship holds

$$\log \rho_r = (3 - D_v) \log (\delta/L) + c \quad (3)$$

with c = constant.

A volume fraction ϕ can be attributed to such an aggregate. The above equation plays an important role in the gelification of e.g. silica particles, which is by nature a percolation process. It has to be taken into account, however, that secondary aggregates of volume fraction ϕ (fractal blobs) and size L and not the primary individual silica particles of diameter δ are the percolating units. Such frail structures may have fractal dimensions below $D_v = 2$. In case of Aerosil 200 aggregates a fractal dimension $D_v = 1.77$ was determined¹³. Thus depending on the structure of an aggregate the range of D_v overlaps the range of linear and surface fractals, introduced in a first step to trigger the imagination. This is not a contradiction, as the definition of linear, surface and volume fractals are arbitrarily related to the Euclidean dimensions to which we are better accustomed. In fact the electron micrograph of an Aerosil aggregate shows a chain-like structure leading to a fractal dimension of

1.77 as already mentioned. Other types may have a fractal dimension close to 2 or even 3. As well known by the work of B. Mandelbrot² the concept of fractal geometry has numerous applications in other fields. In this paper the concept of fractal geometry is treated only in respect to the physics of tablet compaction and the resulting tablet properties.

THE FORMATION OF A TABLET¹⁰

The filling of the die:

For simplicity it is imagined that the volume of the die is spanned by a three-dimensional lattice. The lattice spacing is assumed to be of the order of the mean particle size. If desired, ideal monosized spherical particles can be used. After pouring the particles to be compacted into the die the lattice sites are either occupied by particles or by pores with site occupation probability p . This site occupation probability is equal to the relative density $\rho_r = 1 - \epsilon$ with ϵ = porosity. After application of a minimum of compressional stress the following inequality holds for the particulate system with relative density ρ_r

$$\rho_{cl} < \rho_p < \rho_t < \rho_r \quad (4)$$

with ρ_{cl} = relative density where without action of

gravitational forces, e.g. in a gel the particles form an "infinite" cluster, i.e. bond percolation occurred. The values ρ_p and ρ_t are used to describe the poured and tapped relative densities.

Loose Powder Compacts

To fill hard gelatine capsules one of the principles consists in performing a loose powder compact as a unit dosage form. As only relatively low compressional force is applied, no brittle fracture or plastic flow is expected. However, the relative density $\rho_r > \rho_t$ is sufficient that weak bonds are formed throughout the powder bed. This process can be considered as a bond percolation problem. In addition to the probability p to occupy a lattice site, the bond probability p' has to be introduced. In the thesis of L.E. Holman¹⁴ and a subsequent publication⁷ the bond probability p' was defined as

$$p' = \frac{\rho_r - \rho_t}{1 - \rho_t} \quad (5)$$

i.e. no bonds ($p' = 0$) are expected to be present at the relative tap density ρ_t , and all possible bonds are formed at the relative density $\rho_r = 1$ ($p' = 1$). This model was at that time, however, developed for dense compacts where plastic flow and brittle fracture of

particles can occur. It may be expected that in this site-bond percolation problem all possible weak bonds between the original particles are formed latest before the onset of plastic flow and brittle fracture throughout the whole powder bed. Thus, equation (5) should be modified as follows ("weak-bond" percolation probability p''):

$$p'' = \frac{\rho_r - \rho_t}{\rho_r^* - \rho_t} \quad (6)$$

with ρ_r^* = relative density where brittle fracture or plastic flow become important, i.e. corresponding to a percolation threshold where already an "infinite" cluster of particles exists which shows strong bonds. Because of the non-homogeneity of the stress distribution in a powder bed, isolated agglomerates, which exhibit strong bonding embedded in the loose powder bed, can be expected to be formed at relative densities $\rho_r \geq \rho_s > \rho_t$ but lower than ρ_r^* . Thus a "strong-bond" probability p^* should be defined as

$$p^* = \frac{\rho_r - \rho_s}{1 - \rho_s} \quad (7)$$

with ρ_s = relative density where within the loose powder bed locally strong agglomerates are formed due to the non-homogeneous distribution of compressional stress³. Weak bond probability p'' is in the model (6)

expected to be zero at $\rho_r = \rho_t$. For some substances ρ_t has to be replaced by ρ_p (poured relative density) as $p'' > 0$ for $\rho_r = \rho_t$. According to percolation theory a loose compact of a minimum strength is formed at the bond percolation threshold $p'' = p_c''$. This bond probability p_c'' corresponds to a critical relative density $\rho_c = \rho_b$ for bond percolation. Thus the loose compacts for capsule formulations should show a relative density ρ_r which fulfills the following inequality

$$\rho_p < \rho_t \leq \rho_b < \rho_r < \rho_r^* \quad (8)$$

In this simplified model it is assumed that the particle size of the powdered substances is sufficiently small to form a cohesive compact under a weak compressional stress. In practice the residual moisture content and the individual substance specific capacity to form weaker or stronger bonds have to be taken into account. Thus, microcrystalline cellulose should be able to form relatively loose compacts which show, however, already an adequate strength to be used as tablets.

Dense Powder Compacts

Pharmaceutical Tablets

Tablets represent the majority of solid dosage forms in the pharmaceutical market. This position is

due to its elegance and convenience in application. Thus, a tablet usually has among other properties smooth surfaces, a low friability and a sufficient strength, e.g. tensile strength or deformation hardness. For the production of such tablets the compressional stress σ_c needs to be important enough to induce plastic flow and/or brittle fracture of the primary granules or particles, i.e. to produce simultaneously new surfaces and bonds in this dense powder compact. The critical compressional stress, which is responsible for the onset of plastic flow or brittle fracture throughout the whole powder bed, can be related to the relative density ρ_r^* . Thus the relative density ρ_r of a pharmaceutical compact is usually between ρ_r^* and unity:

$$\rho_r^* < \rho_r < 1 \quad (9)$$

As most of the tablets should show a short disintegration time in the intestinal juices the inequality (9) needs to be closer restricted:

$$\rho_r^* < \rho_r < \rho_\pi < 1 \quad (10)$$

with ρ_π = relative density where the porous system stops being an interpenetrating continuous network of the tablet. Indeed ρ_π corresponds to the (site) percolation threshold of the pores.

The Process of Uniaxial Compression

The usual tabletting machines work according to the principle of uniaxial compression. Thus the upper and lower surface of the tablet remain constant during the compression process, the thickness c of the tablet is reduced with application of the compressional stress σ_z in the z -direction. Because of the initial high porosity of the powder bed the radial transmission σ_r of the main stress cannot be calculated easily. In fact, the principles of continuum mechanics should only be applied for a system with closed pores, i.e. for relative densities $\rho_r > \rho_{\pi}$.

In the following simplified model of uniaxial compression the radial stress σ_r needs not be specified explicitly. However, a lateral displacement or rearrangement of particles occupying former pore sites is allowed. The compression process is now studied starting from a loose powder compact with a relative density ρ_r according to inequality (8). Again a three-dimensional lattice spanning the die volume is imagined. However, a finer grid is assumed with a lattice spacing of the order of the final mean pore size (after compression). According to the principle of uniaxial compression the mean particle-particle distance x is more reduced in the z -direction than in the lateral directions. Thus it can be assumed that in the be-

ginning a one-dimensional bond percolation, i.e. a change from weak to strong bonds in z-direction takes place. Because of non-homogeneous distribution of the compressional stress σ_z along the arrangement and packing of particles and pores in z-direction in the beginning, only selected occupied sites (particles) will be affected and be a part of preformed stronger agglomerates within the still loose powder compact. One can imagine that these affected sites are distributed at random and that their number, i.e. occupation probability p is proportional to the applied compressional stress σ_z .

Thus fig. 1 may represent a computer simulation of randomly affected sites as a projection on two dimensions of surface $a \times b$ of a square-shaped tablet. In this simplified model the uniaxial compression process is reduced essentially to a two-dimensional site percolation phenomenon, associated with a "strong-bond" percolation in three dimensions. It seems to be reasonable that the site percolation is related to the "strong-bond" percolation, i.e. there is a site-bond percolation phenomenon. Thus, the two-dimensional site percolation threshold $p_c = \rho_r^*$ (site percolation probability p) should roughly correspond to the three-dimensional "strong-bond" percolation threshold

$$p_c^* = \frac{\rho_r^* - \rho_s}{1 - \rho_s} \quad (11)$$

At a certain compressional stress σ_z^* an infinite cluster of rigid "strong-bond" particles is formed, i.e. there is a site percolation threshold which corresponds to a certain relative density ρ_r^* . At this relative density the compact can be considered as the "first" dense tablet. At this percolation threshold the particles can also no longer be easily displaced into a lateral direction. However, lateral stress transmission to the die walls will become important. In a powder bed the packing of the particles, the size and shape factors are usually not known accurately. However, a coordination number k can be estimated from the porosity¹² $\epsilon = 1 - \rho_r$ as mentioned earlier.

Thus it is possible to relate the experimentally determined percolation threshold p_c with the estimated coordination number k and to compare these values with the theoretical values in table 2.

Stress Transmission in the Die

It is well known that the compressional stress is transmitted from the upper punch to the lower punch by means of particle-particle contact in the powder bed. Thus, one may expect that the stress is conducted similar to electric current. As a consequence it is of interest to measure at the same time the stress and the

TABLE 3

Physical Characterization of Aerosil 200 and different Types of Carbon Black

| Material | BET surface (m ² /g) | Density (g/cm ³) | | | Fractal Dimension |
|---------------------------|------------------------------------|------------------------------|--------|--------|----------------------|
| | | true | poured | tapped | |
| Aerosil 200 | 202 | 2.2 | 0.016 | 0.022 | 1.77 ± 0.05 |
| Types of Carbon Black: | | | | | |
| Noir d'acé- tylène | 80 | 1.87 | 0.027 | 0.041 | 1.99 ± 0.10 |
| TB # 4500 | 57 | 1.83 | 0.043 | 0.066 | 1.76 ± 0.12 |
| TB # 5500 | 206 | 1.84 | 0.025 | 0.043 | 1.83 ± 0.13 |
| Sterling FT | 15 | 1.85 | 0.27 | 0.40 | 3.0 |

electric current transmitted. This experimental work was realized by F. Ehrburger¹³ et al. using as a conducting material different types of Carbon Black and for comparison the electrical insulating silica particles Aerosil 200. The physical characterization of the material tested is compiled in table 3.

Silica was chosen because this material is often used to study the gelation process which can be adequately described by percolation theory. Using a non-linear regression analysis the parameters of the following power laws were determined

$$C = C_0 (\rho_r - \rho_c)^t \quad (12)$$

$$\sigma_c = \sigma_o (\rho_r - \rho_o)^\tau \quad (13)$$

with C = Conductivity $[(\text{ohm cm})^{-1}]$, C_o = Scaling factor
 σ_c = compressional stress transmitted, σ_o = Scaling factor and t , τ = conductivity exponent, which is expected to be close to 2.

The results of this investigations are compiled in table 4.

From table 4 it can be concluded that both the stress transmission and the conductivity follow the power laws of percolation. The value of ρ_{\max} should indicate the range of relative densities ρ_r : $\rho_o < \rho_r < \rho_{\max}$ and $\rho_c < \rho_r < \rho_{\max}$ where this power law is still valid. Table 4 shows rather low values for the

TABLE 4

Stress Transmission and Conductivity of Aerosil 200 and different types of Carbon Black

| Material | Stress Transmission | | | Conductivity | | |
|------------------------|---------------------|---------|---------------|--------------|---------|---------------|
| | ρ_o | τ | ρ_{\max} | ρ_c | t | ρ_{\max} |
| Aerosil 200 | 0.025 | 1.5±0.1 | 0.06 | - | - | - |
| Types of Carbon Black: | | | | | | |
| Noir d'acétylène | 0.032 | 2.9±0.1 | >0.24 | 0.024 | 1.9±0.1 | ≥0.24 |
| TB # 4500 | 0.050 | 2.2±0.1 | 0.15 | 0.040 | 1.8±0.1 | ≥0.27 |
| TB # 5500 | 0.033 | 2.1±0.1 | 0.10 | 0.019 | 1.8±0.1 | >0.2 |
| Sterling FT | 0.27 | 3.9±0.2 | >0.56 | 0.27 | 3.4±0.2 | >0.56 |

percolation thresholds ρ_0 respectively ρ_c . This fact can be explained that in the process of percolation secondary agglomerates (aggregates of size L) consisting of primary carbon black or silica particles (of size δ) are responsible for the stress transmission. Taking into account the fractal geometry of these aggregates F. Ehrburger¹³ et al. obtained a good estimate for the ratio L/δ using the following equation

$$\rho_0 = 0.17 (L/\delta)^{D-3} \quad (14)$$

The values calculated for L/δ were in good agreement with estimates obtained from independent experiments (BET- and porosimetry measurements).

TABLET PROPERTIES

A number of tablet properties are directly or indirectly related to the relative density ρ_r of the compact. According to percolation theory the following relationship holds for the tablet property X close to the percolation threshold p_c

$$X = A (p - p_c)^q \quad (15)$$

X = tablet property

p = percolation probability

p_c = percolation threshold

A = scaling factor

q = exponent

In case of a tablet property X the values of A and q are not known a priori. In addition the meaning of p and p_c has to be identified individually for each property X . As mentioned earlier the percolation probability p is in a site percolation problem identical with the relative density ρ_r . For obvious reasons one can expect that the tensile strength σ_T and the deformation hardness P are related to the relative density ρ_r as follows

$$\sigma_T = A_T (\rho_r - \rho_c)^{q_T} \quad (16)$$

and
$$P = A_P (\rho_r - \rho_c)^{q_P} \quad (17)$$

Unfortunately, in a practical case only the experimental values of σ_T , P and ρ_r of the tablet are known. In this respect, it is important to take into account the properties of the power law (equation 15) derived from percolation theory: 1) the relationship holds close to the percolation threshold but it is unknown in general how close, 2) the a priori unknown percolation threshold p_c and the critical exponent q are related. Thus there is a flip-flop effect between p_c and q , a low p_c value is related to a high q value and vice versa. As a consequence the data evaluation

TABLE 5

Percolation Exponents for two Dimensions, three Dimensions and in the Bethe Lattice together with the corresponding Quantity¹

| Exponent | d=2 | d=3 | Bethe | Quantity |
|----------|-------|------|-------|------------------------------|
| α | -2/3 | -0.6 | -1 | Total number of clusters |
| β | 5/36 | 0.4 | 1 | Strength of inf. network |
| γ | 43/18 | 1.8 | 1 | Mean size of finite clusters |
| ν | 4/3 | 0.9 | 1/2 | Correlation length |
| μ | 1.3 | 2.0 | 3 | Conductivity |

based on non-linear regression analysis to determine A , p_c and q may become very tedious or even impossible.

In selected cases such as percolation in a Bethe lattice the percolation exponent q is equal to unity. A list of selected exponents for 2, 3 and infinite dimensions (i.e. Bethe lattice) known from first principles is compiled in table 5 and cited from D. Stauffer¹. Details should be read there concerning the relevant equation for the property of the system described.

In case of the tablet properties such as tensile strength σ_T and deformation hardness P no meaningful results can be obtained without taking additional expertise. It was a rewarding endeavour¹⁰ to combine the following two equations derived earlier¹⁵ with the well-known Heckel equation¹⁶.

$$\sigma_T = \sigma_{Tmax} (1 - e^{-\gamma \sigma_c \rho_r}) \quad (18)$$

$$P = P_{max} (1 - e^{-\gamma \sigma_c \rho_r}) \quad (19)$$

and

$$\ln \frac{1}{1 - \rho_r} = a + b \sigma_c \quad (20)$$

This derivation does not take into account the exact value of ρ_r (usually between 0.6 and 1) in the exponent of the equations (18) and (19). The combination of equations (18) and (20) respectively (19) and (20) yielded the following relationships

$$\sigma_T = \frac{\sigma_{Tmax}}{1 - \rho_r^*} (\rho_r - \rho_r^*) \quad (21)$$

$$P_{max} = \frac{P_{max}}{1 - \rho_r^*} (\rho_r - \rho_r^*) \quad (22)$$

with ρ_r^* = critical relative density (percolation threshold). Due to the compaction properties of different types of particulate matter, critical relative densities for the formation of loose and dense compacts could be determined. The percolation exponent is in the equations equal to unity and corresponds to a percolation in a Bethe lattice¹. The experimental methods and data evaluation are described in detail in a recent paper¹⁰. The percolation thresholds were

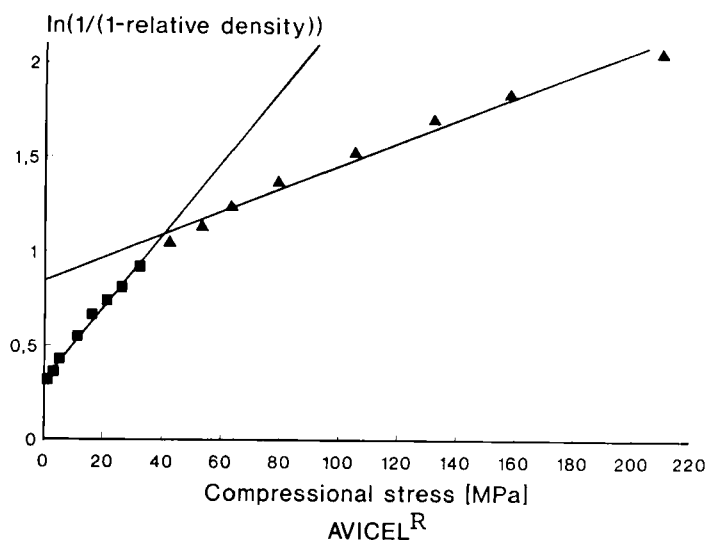


FIGURE 5

Heckel-plot of microcrystalline cellulose (Avicel^R) in order to determine the percolation thresholds for loose and dense compacts (ρ_t and ρ_r^*).

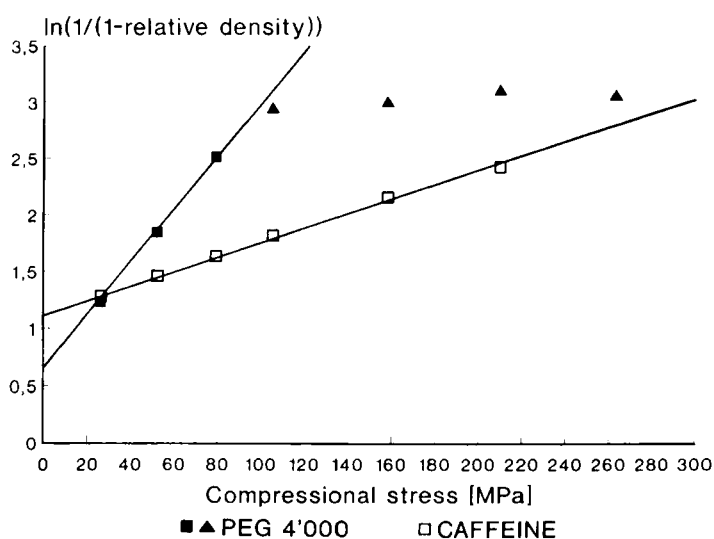


FIGURE 6

Heckel-plot of PEG 4000 and caffeine anh. in order to determine the percolation thresholds for dense powder compacts (ρ_r^*).

TABLE 6

Results according to Equations (21) and (22)

| Substance | | $\sigma_{Tmax} \pm SD [MPa]$ | r | $P_{max} \pm SD [MPa]$ | r |
|--------------------------|----|------------------------------|-------|------------------------|-------|
| Avicel ^R | I | 3.04±0.43 | 0.955 | 34.92± 2.11 | 0.990 |
| | II | 12.94±1.53 | 0.984 | 102.39±14.05 | 0.970 |
| Caffeine | | 3.71±0.37 | 0.998 | 270.09±36.00 | 0.983 |
| Emcompress ^R | I | 0.15±0.02 | 0.979 | 5.56± 1.42 | 0.917 |
| | II | 1.39±0.13 | 0.983 | 109.49±21.60 | 0.931 |
| PEG 4'000 | | 2.52±0.96 | 0.989 | 57.50±21.25 | 0.994 |
| PEG 10'000 | | 3.22±1.32 | 0.983 | 58.02±23.27 | 0.986 |
| | | 2.11±0.37 | 0.961 | 8.81± 1.27 | 0.975 |
| Lactose | I | 0.37±0.09 | 0.894 | 13.14± 2.37 | 0.939 |
| | II | 2.52±0.56 | 0.964 | 81.02±17.67 | 0.966 |
| | | 2.67±0.64 | 0.970 | 318.12±74.69 | 0.972 |
| <hr/> | | | | | |
| I Loose powder compacts | | | | | |
| II Dense powder compacts | | | | | |

determined on the basis of the Heckel equation (see figs. 5 and 6). The results of the equations (21) and (22) are compiled in table 6. Typical plots are shown in figs. 7 - 10.

The description of other tablet properties such as disintegration time³, dissolution rate etc. according to percolation theory are limited as long as not the theoretical models are established to know more about the respective percolation exponents. However, in the special case of a matrix type slow release system^{8,9} it is possible to apply simultaneously the concept of

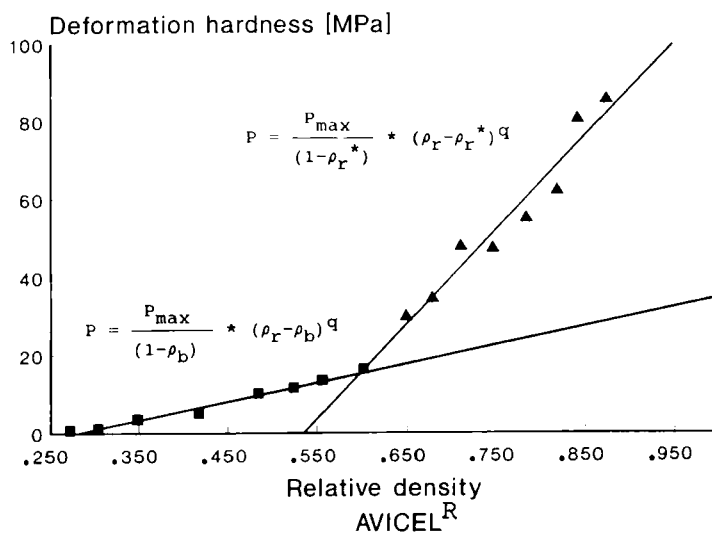


FIGURE 7

Tablet property: Deformation hardness of Avicel^R compacts as a function of relative density according to percolation theory (power law).

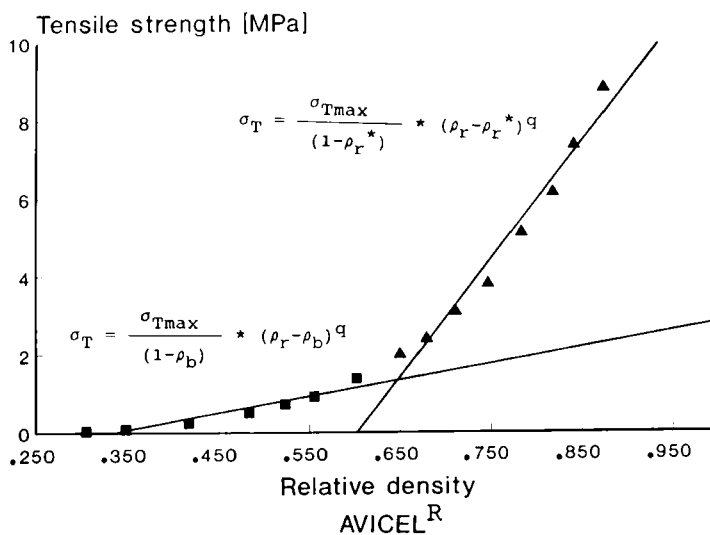


FIGURE 8

Tablet property: Tensile strength of Avicel^R compacts as a function of relative density according to percolation theory (power law).

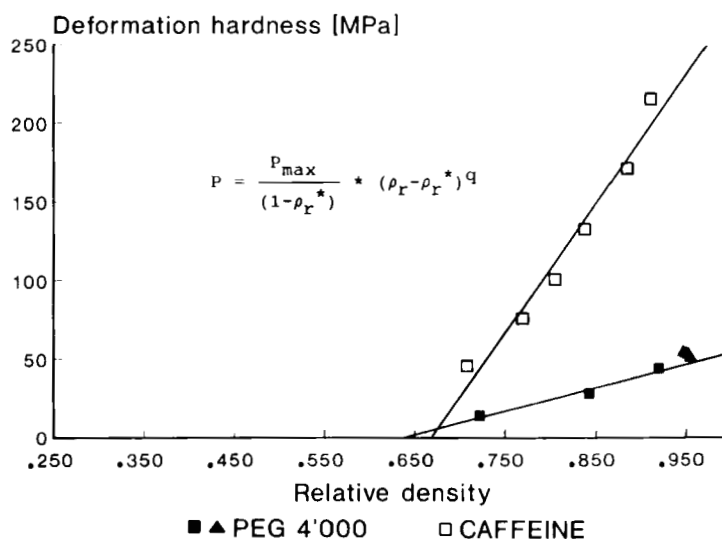


FIGURE 9

Tablet property: Deformation hardness of PEG 4000 and caffeine compacts as a function of relative density according to percolation theory (power law).

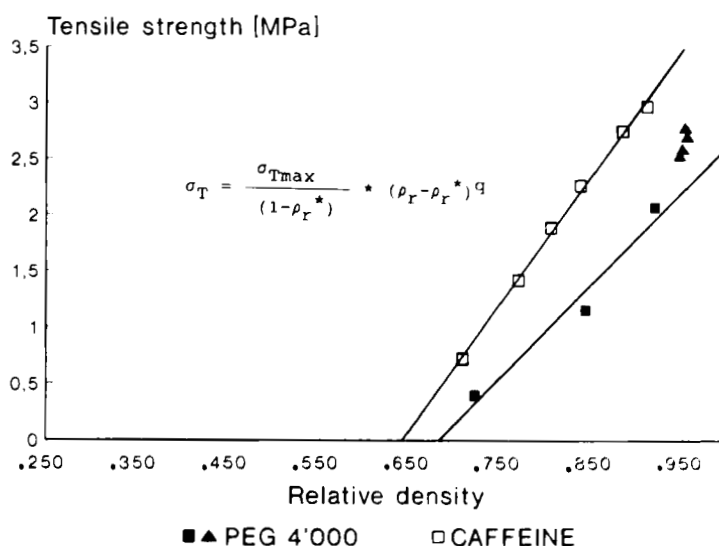


FIGURE 10

Tablet property: Tensile strength of PEG 4000 and caffeine compacts as a function of relative density according to percolation theory (power law).

percolation theory and fractal geometry. This is the topic of the next chapter¹⁷.

DRUG DISSOLUTION FROM A MATRIX TYPE CONTROLLED RELEASE SYSTEM

Ants in a labyrinth and drug dissolution kinetics

Molecules of an active substance, which are enclosed in a matrix type controlled release system, may be called ants in a labyrinth¹ trying to escape from an ordered or disordered network of connected pores. The random walk distance R of such an ant is related to time as follows: $R^2 = Dt$, where D is equal to the diffusivity. Close to the percolation threshold, where the pores start to form isolated clusters, this diffusion law is not valid. In this case the value of D varies proportionally to $(p - p_c)^\mu$, where μ is the conductivity exponent and R is proportional to t^k with $k = 0.27$. This process is called anomalous diffusion.

From these first principles one can conclude that there is at least one percolation threshold, i.e. the percolation threshold p_c , where the active drug is completely encapsulated by the water-insoluble matrix substance and that the usual square-root-of-time law for the dissolution kinetics is no longer valid. As in

general, in a three-dimensional system two percolation thresholds can be expected and an experiment was set-up to elucidate more in detail this phenomenon. For this purpose, a well water-soluble model drug (Caffeine anhydrous) and a plastic water-insoluble matrix substance (Ethylcellulose) were chosen. The materials and methods used are described in detail in a recent publication¹⁷ and should be read there. Thus in this paper only the theoretical background and the conclusions are summarized. In this experiment the drug content was varied from 10% to 100% (w/w) and the drug dissolution from one flat side of the tablets was studied. For this purpose the tablet was fixed into a paraffin matrix to leave only one side of the tablet accessible for the dissolution medium (distilled water).

For low drug concentrations, i.e. low porosity of the matrix, most of the drug will be encapsulated by the plastic matrix and the release will be incomplete. At the lower percolation threshold p_{C1} the drug particles begin to form a connective network within the matrix and the diffusion will be anomalous just at the threshold. At the upper percolation threshold p_{C2} the particles which should form a matrix start to get isolated within the drug particles and the tablet would disintegrate.

The concentration of the drug particles within the matrix can be expressed as site percolation probability p . The amount of drug $Q(t)$ released from one tablet surface after the time t is proportional to t^k and the exponent k depends on the percolation probability p :

- Case 1: $p < p_{C1}$: Only the few particles connected to the tablet surface can be dissolved and $Q(t)$ reaches a constant value.
- Case 2: $p \approx p_{C1}$: Anomalous diffusion with $k \approx 0.2$ in three dimensions¹, range of $p \approx p_{C1} \pm 0.1 p_{C1}$ approximately.
- Case 3: $p_{C1} < p < p_{C2}$: Normal matrix-controlled diffusion with $k = 0.5$.
- Case 4: $p > p_{C2}$: Zero order kinetics with $k = 1$.

Between the two percolation thresholds p_{C1} and p_{C2} the particles of drug and matrix substance form a bicoherent system, i.e. the drug release matches the well-known square-root-of-time law of Higuchi¹⁸ for porous matrices:

$$Q(t) = \sqrt{\frac{D_0 \epsilon}{\tau} C_S (2A - \epsilon C_S) t} = \sqrt{D C_S (2A - \epsilon C_S) t} \quad (23)$$

with Q = cumulative amount of drug released per unit exposed area

D_o = diffusion coefficient of the drug in the permeating fluid

ϵ = total porosity of the matrix (carcass)

τ = tortuosity of the matrix

C_s = solubility of the drug in the permeating fluid

A = concentration of the dispersed drug in the tablet

D = apparent or observed diffusion coefficient

Close to the percolation threshold the observed diffusion coefficient obeys a scaling law which can be written as follows¹:

$$D \text{ prop. } (p - p_{c1})^\mu \quad (24)$$

with p = site percolation probability

p_{c1} = critical percolation probability (lower percolation threshold)

μ = conductivity exponent = 2.0 in three dimensions¹ (see table 5).

In the case of a porous matrix p can be expressed by the total porosity ϵ of the matrix or carcass and p_{c1} corresponds to a critical porosity ϵ_c , where the pore network just begins to span the whole matrix. Equation (24) can then be written as:

$$D \propto (\epsilon - \epsilon_c)^\mu$$

or

$$D = \kappa D_0 (\epsilon - \epsilon_c)^\mu \quad (25)$$

with κD_0 = scaling factor.

In the cases where the dissolution kinetics are in agreement with equation (23) the dissolution data can be linearized by plotting $Q(t)$ versus \sqrt{t} giving a regression line with the slope b .

$$b = \sqrt{D C_S (2 A - \epsilon C_S)}$$

which leads to

$$D = \frac{b^2}{C_S (2 A - \epsilon C_S)} \quad (26)$$

Combining equations (25) and (26) and assuming $\mu = 2.0$ results in:

$$\frac{b^2}{C_S (2 A - \epsilon C_S)} = \kappa D_0 (\epsilon - \epsilon_c)^\mu$$

or

$$X = \frac{b}{\sqrt{2 A - \epsilon C_S}} = \sqrt{\kappa D_0 C_S} (\epsilon - \epsilon_c) \quad (27)$$

i.e. the tablet property X is determined by a linear relationship of ϵ :

$$X = c (\epsilon - \epsilon_c) = -c\epsilon_c + c\epsilon \quad (28)$$

where the constant c equals $\sqrt{\kappa D_0 C_S}$.

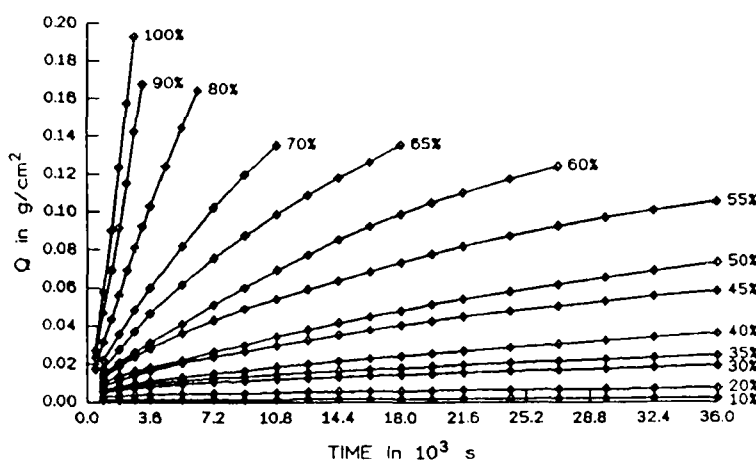


FIGURE 11

Cumulative amount $Q(t)$ of caffeine per unit area released as a function of time for tablets with caffeine loadings between 10% (w/w) and 100% (w/w).

By the help of equation (28) ϵ_c can easily be calculated by using a non-linear or even a linear regression analysis, giving a slope of c and an intercept of $-c\epsilon_c$.

The results of the intrinsic dissolution test of the tablets with the different caffeine loadings are plotted in fig. 11. A change in dissolution kinetics can be assumed between 70% and 80% of caffeine loading. In order to check this assumption the release data are evaluated according to the model $Q(t) = a + b\sqrt{t}$ by a simple linear regression to clarify for which loadings the square-root-of-time law is fulfilled. To clear up the diffusion mechanism the data are also evaluated

TABLE 7

Evaluation of Dissolution Data and Percolation Thresholds

| Drug content | $Q(t) = a + \frac{b\sqrt{t}}{r^2}$ | | $Q(t) = a' + \frac{b't^k}{r^2}$ | |
|--------------------------------------|------------------------------------|--------|---------------------------------|---------|
| 10 | 0.006 | 0.9858 | 0.17 | 0.9615 |
| 20 | 0.027 | 0.9975 | 0.27 | 0.9932 |
| Lower percolation threshold expected | | | | |
| 30 | 0.085 | 0.9989 | 0.37 | 0.9983 |
| 35 | 0.116 | 0.9994 | 0.41 | 0.9973 |
| 40 | 0.189 | 0.9954 | 0.52 | 0.9963 |
| 45 | 0.320 | 0.9987 | 0.54 | 0.9992 |
| 50 | 0.415 | 0.9929 | 0.61 | 0.9980 |
| 55 | 0.593 | 0.9989 | 0.56 | 0.9979 |
| 60 | 0.858 | 0.9936 | 0.67 | 0.9979 |
| 65 | 1.15 | 0.9983 | 0.66 | 0.9991 |
| 70 | 1.56 | 0.9941 | 0.74 | 0.9996 |
| Upper percolation threshold expected | | | | |
| 80 | 2.55 | 0.9863 | 0.84 | 0.9998 |
| 90 | 4.11 | 0.9752 | 1.02 | 0.9991 |
| 100 | 5.38 | 0.9784 | 1.09 | >0.9999 |

Drug content in % (w/w)

 b = slope in $10^{-3} \text{g} \cdot \text{cm}^{-2} \cdot \text{s}^{-1/2}$ k = dimensionless exponent r^2 = squared correlation coefficient

according to $Q(t) = a' + \frac{b't^k}{r^2}$ by a nonlinear least square fit. The results are compiled in table 7.

Comparing the squared correlation coefficients of the \sqrt{t} - evaluation, there is a clear decrease in the grade of correlation for caffeine loadings higher than 70%, i.e. the drug loadings from 80% to 100% caffeine are no longer in good agreement with the \sqrt{t} -law. For low drug concentrations only a small amount of drug is

released and the dissolution curve runs nearly parallel to the abscissa. In these cases the correlation coefficient cannot be used as an indicator for the compliance with the model.

The estimation of k according to the model $Q(t) = a' + b't^k$ yields values for k between 0.17 and 1.09. For 35% to 55% of caffeine the exponent k ranges between 0.41 and 0.61, which is in good agreement with the \sqrt{t} -kinetics with $k = 0.5$. For higher loadings there is a clear change from \sqrt{t} -kinetics to zero order kinetics with $k = 1$. Both evaluations show that the upper percolation threshold p_{C2} lies between 70% and 80% of caffeine.

For the quantitative determination of the lower percolation threshold p_{C1} , i.e. the critical porosity ϵ_c , equations (27) and (28) are used. The needed data are summarized in table 8.

The initial porosity ϵ_o before evaluation is calculated from the apparent volume V_{tot} and the true volume V_t of the tablet:

$$\epsilon_o = \frac{V_{tot} - V_t}{V_{tot}} \quad (29)$$

ϵ_d is the porosity corresponding to the volume occupied by the drug substance in the matrix calculation as

TABLE 8

Calculation of D and the Tablet Property X

| Drug content | ϵ_0 | ϵ_d | ϵ | A | b | D | X |
|--------------|--------------|--------------|------------|-------|-------|--------|-------|
| 10 | 0.134 | 0.078 | 0.212 | 0.110 | 0.006 | 0.0045 | 0.013 |
| 20 | 0.128 | 0.158 | 0.286 | 0.225 | 0.027 | 0.0437 | 0.041 |
| 30 | 0.121 | 0.242 | 0.363 | 0.344 | 0.085 | 0.282 | 0.104 |
| 35 | 0.118 | 0.285 | 0.403 | 0.405 | 0.116 | 0.446 | 0.130 |
| 40 | 0.116 | 0.328 | 0.444 | 0.466 | 0.189 | 1.03 | 0.198 |
| 45 | 0.109 | 0.375 | 0.484 | 0.532 | 0.320 | 2.58 | 0.313 |
| 50 | 0.110 | 0.418 | 0.528 | 0.594 | 0.415 | 3.88 | 0.384 |
| 55 | 0.106 | 0.465 | 0.571 | 0.660 | 0.593 | 7.13 | 0.520 |
| 60 | 0.103 | 0.512 | 0.615 | 0.727 | 0.858 | 13.5 | 0.717 |
| 65 | 0.098 | 0.562 | 0.660 | 0.798 | 1.15 | 22.2 | 0.918 |
| 70 | 0.099 | 0.608 | 0.707 | 0.863 | 1.56 | 37.7 | 1.197 |
| 80 | 0.092 | 0.708 | 0.800 | 1.006 | 2.55 | 86.4 | 1.811 |
| 90 | 0.088 | 0.811 | 0.899 | 1.151 | 4.11 | 196 | 2.729 |
| 100 | 0.080 | 0.920 | 1.000 | 1.306 | 5.38 | 296 | 3.353 |

Drug content in % (w/w)

 ϵ_0 = initial tablet porosity ϵ_d = porosity due to drug content ϵ = total porosity of matrixA = concentration of dispersed drug in tablet in g/cm^3 b = slope in $10^{-3} \text{ g} \cdot \text{cm}^{-2} \cdot \text{s}^{-1/2}$ D = apparent diffusion coefficient in $10^{-6} \text{ cm}^2/\text{s}$ X = tablet property in $10^{-3} \text{ g}^{1/2} \cdot \text{cm}^{-1/2} \cdot \text{s}^{-1/2}$

follows:

$$\epsilon_d = \frac{m_d}{\rho_d V_{\text{tot}}} \quad (30)$$

with m_d = total amount of drug present in the tabletand ρ_d = true density of drug. ϵ is the total porosity of the matrix (carcass):

$$\epsilon = \epsilon_0 + \epsilon_d \quad (31)$$

D is calculated according to equation (26) and the tablet property X to equation (27).

For estimating ϵ_c with the help of equation (28) the data for ϵ and X for 35% to 55% of caffeine are used, because in this range there is the best agreement with the normal diffusion law, i.e. \sqrt{t} -kinetics with $k = 0.5$ (see table 8). The nonlinear regression yields $\epsilon_c = 0.35 \pm 0.01$ and $c = (2.30 \pm 0.15) 10^{-3} \text{ g}^{1/2} \cdot \text{cm}^{-1/2} \cdot \text{s}^{-1/2}$. A linear regression analysis leads to the same result. The critical porosity of 0.35 corresponds to a caffeine content of about 28% (weight/weight). Fig. 12 shows the plot of X versus ϵ where the point of intersection with the abscissa just indicates ϵ_c .

In table 1 selected percolation thresholds¹ for three-dimensional lattices (as volume-to-volume ratios) and in table 2 the corresponding coordination numbers¹⁹ for isometric spherical particles are compiled. Comparing the experimentally determined percolation threshold of 0.35 (volume-to-volume ratio) with the theoretical values shows a good agreement with the simple cubic lattice, which has a site percolation threshold of 0.312. In the tablet a brittle and a plastic substance of different grain size are compacted together so that the postulation of a lattice composed of isometric spheres is only a rough estimate, but it points out that the magnitude of the found ϵ_c is reasonable.

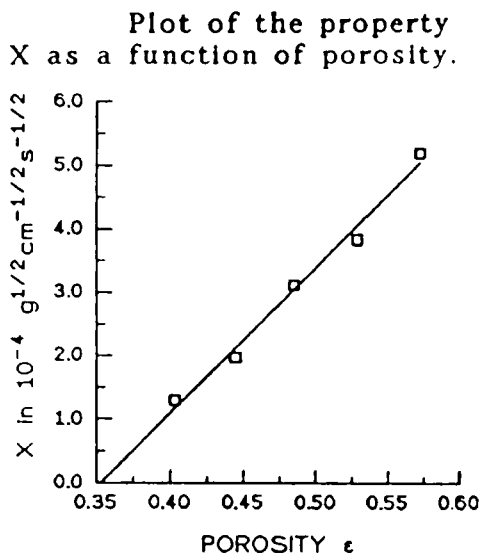


FIGURE 12

Tablet property X as a function of porosity ϵ (power law) according to percolation theory.

Fractal Dimension of a Pore System of a Matrix Type Slow Release System

If the matrix type slow release dosage form of the preceeding chapter is removed from the dissolution medium after e.g. a maximum of 60% (w/w) of drug dissolved to guarantee the physical stability of the remaining carcass, the open pore system left can be analysed by mercury intrusion porosimetry to determine the fractal dimension. It is evident that the pore structure depends on the particle size distribution of the brittle model drug caffeine anhydrous originally

embedded into the plastic Ethocel^R matrix. The fractal dimensions⁹ of the leached tablets ranged between 2.67 and 2.837 depending on the particle size distribution of the water-soluble drug. The system which contained the broad fraction (125-355 μm) yielding a fractal dimension of 2.734 was closest to the dimension of the Menger sponge ($D = 2.727$).

Fractal Dimension of the Porous Network of a Fast Disintegrating Tablet

In the thesis of Bernhard Luy²⁰ tablets were produced from granules which showed a very high porosity and internal surface. Those granules were obtained with a novel process technology: vacuum fluidized-bed spray granulation^{21,22}. Independent of the granule size distribution the resulting tablets released 100% of the soluble drug (solubility in water < 0.01%) within 5 minutes. The disintegration time was smaller than 1 minute. The fractal dimension of the porous network ranged from 2.82 to 2.88.

CONCLUSIONS

The concept of percolation theory and fractal geometry allowed new insights into the physics of tablet compaction and the properties of the tablets. The

results attained so far are promising and should stimulate further research in this field.

REFERENCES

- [1] D. Stauffer, "Introduction to Percolation Theory", Taylor and Francis, London and Philadelphia, 1985.
- [2] B.B. Mandelbrot, "The Fractal Geometry of Nature", Freeman, San Francisco, 1982.
- [3] H. Leuenberger, B.D. Rohera and C. Haas, Int. J. Pharm., 38, 109 (1987).
- [4] L.E. Holman and H. Leuenberger, Int. J. Pharm., 46, 35 (1988).
- [5] H. Leuenberger, L.E. Holman, M. Usteri and S. Winzap, Pharm. Acta Helv., 64, 34 (1989).
- [6] D. Blattner, M. Kolb and H. Leuenberger, Pharm. Res., 7, 113 (1990).
- [7] L.E. Holman and H. Leuenberger, "The significance of slopes of the semilogarithmic relationship between hardness and solid fraction of porous compacts", Powder Technol. (in press).
- [8] H. Leuenberger, J.D. Bonny and M. Usteri, "Particle Size Effects on Fractal Dimension of Matrix Type Slow-Release Systems", Proceed. of Second World Congress Particle Technology, Sept. 19-22, 1990, Kyoto, Japan.
- [9] M. Usteri, J.D. Bonny and H. Leuenberger, Pharm. Acta Helv., 65, 55 (1990).
- [10] H. Leuenberger and R. Leu, "The Formation of a Tablet: A site-bond percolation phenomenon", paper submitted.
- [11] J.D. Bonny and H. Leuenberger, "Percolation Effects in Controlled Release Matrices", paper submitted.

- [12] W.O. Smith, P.D. Foote and P.F. Busang, *Phys. Rev.*, 34, 1272 (1929).
- [13] F. Ehrburger, S. Misono et J. Lahaye "Percolation dans les poudres de noirs de carbone" in "Conducteurs granulaires, théories, caractéristiques et perspectives", journée d'études Oct.10, 1990, Paris, Textes de communication p. 197-204.
- [14] L.E. Holman, PhD-Thesis, University of Basel, 1988.
- [15] H. Leuenberger, *Int. J. Pharm.*, 12, 41 (1982).
- [16] R.W. Heckel, *Transactions of the Metallurgical Society of AIME*, 221, 671 (1961).
- [17] J.D. Bonny and H. Leuenberger, "Matrix Type Controlled Release Systems: Effect of Percolation on Drug Dissolution Kinetics", paper submitted *Pharm. Acta Helv.*
- [18] T. Higuchi, *J. Pharm. Sci.*, 52, 1145 (1963).
- [19] P.J. Sherrington and R. Oliver, "Granulation", Heyden, London 1981, p. 34.
- [20] Bernhard Luy, PhD-thesis, University of Basel, 1991.
- [21] B. Luy, P. Hirschfeld and H. Leuenberger, *Drugs made in Germany*, 32, 68 (1989).
- [22] H. Leuenberger, B. Luy and P. Hirschfeld, "Experiences with a novel fluidized bed system operating under vacuum conditions", in *Proceed. of the Preworld Congress Particle Technology*, Sept. 17-18, 1990, Gifu, Japan.